Self-Assembly and Critical Solubility Temperature of Supramolecular Polystyrene Bottle-Brushes in Cyclohexane

Sylvain Catrouillet, Laurent Bouteiller, Erwan Nicol, Taco Nicolai, Sandrine Pensec, Boris Jacquette, Maël Le Bohec, Olivier Colombani

Self-Assembly and Critical Solubility Temperature Of Supramolecular Polystyrene Bottle-Brushes In Cyclohexane

Sylvain Catrouillet[a], Laurent Bouteiller[b], Erwan Nicol[a], Taco Nicolai[a], Sandrine Pensec[b], Boris Jacquette[a], Maël Le Bohec[a] and Olivier Colombani[a,]*

[a] LUNAM Université, Université du Maine, IMMM – UMR CNRS 6283, Université du Maine, av. O. Messiaen, 72085 Le Mans cedex 9, France.

[b] Sorbonne Université, UPMC Univ Paris 06, UMR 8232, IPCM, Chimie des Polymères,F-75005 Paris, France, and CNRS, UMR 8232, IPCM, Chimie des Polymères, 75005 Paris, France

KEYWORDS. Self-assembly, urea, comb polymer, phase separation, phase diagram, cloud point, anisotropic nanoparticle, cylinder.

ABSTRACT.

The formation of polystyrene (PS) supramolecular bottle-brushes by self-assembly in cyclohexane of hydrogen-bonding trisurea units decorated by PS chains was investigated using light and neutron scattering. Atom Transfer Radical Polymerization (ATRP) was used to control the length of the PS side-chains and allowed the straightforward synthesis of the targeted trisureas. It was shown that their extent of self-assembly strongly depended on the degree of polymerization and

chemical nature of the polymer side chains, in contrast with what was previously observed with cyclic oligopeptides, another type of self-assembling units. With sufficiently short PS side-chains, anisotropic supramolecular bottle-brushes could be obtained. Their critical solubility temperature, T_c, was measured in cyclohexane, proving experimentally for the first time that densely grafted PS bottle-brushes exhibit a much lower T_c than linear PS or even star-shaped PS of similar molecular weight.

Introduction

Supramolecular chemistry is a powerful bottom-up approach which allows the formation of complex structures by self-assembly of much simpler molecules through non covalent interactions.[1-5] In this context, the design of bottle-brush polymers using non covalent bonds has been the subject of growing interest because covalent bottle-brush polymers, consisting of a backbone decorated by densely grafted side-chains, are not easy to obtain by conventional synthetic methods.[6-8] Efforts have therefore been made to connect the side-chains to the backbone by non covalent interactions[9, 10] or more recently to form the backbone itself by supramolecular directional interactions.[11] In the latter case, the non covalent growth of the backbone, decorated by polymer side-chains, has been promoted by self-assembly of shape persistent macrocycles through π-stacking[12-17] or by self-assembly through hydrogen bonding of cyclic oligopeptides,[11, 18-35] linear oligopeptides[36] or, more recently, urea-based self-assembling units[37-39].

Polymer arms of different nature have been connected to the self-assembling units in order to tune the solubility of the resulting bottle-brush,[28] impart some functionality to it,[40] or prepare Janus particles.[40] Very few reports relate the effect of the degree of polymerization and chemical nature of the polymer arms on the extent of self-assembly, which would be required to know how to

control the length of the bottle-brushes.[20, 22, 25, 27] Rather surprisingly, the extent of self-assembly of cyclic oligopeptides is only little influenced by the degree of polymerization of the side chains[20, 22] and almost not influenced by their chemical nature.[22] To the best of our knowledge, no studies have been made in this context on urea-based supramolecular bottle-brushes.

We report here the synthesis and characterization by controlled radical polymerization of two trisureas decorated by PS arms of different number average degrees of polymerization (DP_n): $S_{34}U_3S_{34}$ (DP_n = 34) and $S_{14}U_3S_{14}$ (DP_n = 14). The degree of polymerization of the arms of $S_{34}U_3S_{34}$ was chosen to allow direct comparison with U3PIB2, a polyisobutylene-decorated trisurea previously studied[38] whose arms have a similar degree of polymerization (DP_n = 27). The self-assembly of $S_{34}U_3S_{34}$ and $S_{14}U_3S_{14}$ was studied by scattering techniques in cyclohexane, a solvent in which the solubility of PS strongly depends on the temperature.[41] The aim of this work was twofold. First, we investigated for the first time the influence of the chemical nature and degree of polymerization of the arms on the self-assembly of trisurea-based bottle-brushes, revealing large differences of behavior compared to cyclic oligopeptides. Second, we showed experimentally for the first time that a bottle-brush architecture has a strong effect on the critical solubility temperature, T_c, of PS in cyclohexane.

Materials and Methods

All experimental details concerning the synthesis of $S_{14}U_3S_{14}$ and $S_{34}U_3S_{34}$ are given in Supporting Information.

Preparation of the solutions.

Stock polymer solutions of $S_{14}U_3S_{14}$ and $S_{34}U_3S_{34}$ in cyclohexane were prepared at 1, 10 or 100 g/L by direct dissolution of either polymer at room temperature. Both polymers dissolved

spontaneously under stirring at room temperature and the solutions could be filtered through 0.2 μm pore size Acrodisc filters 12 hours after their preparation. Dilutions were obtained by adding filtered solvents (0.02 μm) and stirring for a few minutes. The solutions were heated at 60 °C during 1 hour just before being measured in order to obtain stable solutions more quickly. They remained stable for weeks after preparation. Solutions directly prepared at 10 g/L gave the same results as solutions diluted to 10 g/L from a stock solution at 100 g/L.

Light scattering. Light scattering measurements were done using an ALV-CGS3 system operating with a vertically polarized laser with wavelength λ=632 nm (ALV-GmbH, Langen, Germany). The measurements were done at 50°C over a range of scattering wave vectors ($q=4\pi n.\sin(\theta/2)/\lambda$, with θ the angle of observation and n the refractive index of the solvent) varying from 4.8×10^{6} m^{-1} to 2.8×10^{7} m^{-1}.

Dynamic Light Scattering (DLS). The normalized electric field autocorrelation functions ($g_1(t)$) obtained by dynamic light scattering (DLS) measurements were analysed in terms of a relaxation time distribution ($A_{(\tau)}$) :

$$g_1(t) = \int A_{(\tau)} \exp\left(-t/\tau\right) d\tau \qquad \text{equation 1}$$

All correlograms could be well described by a log-normal distribution. The average relaxation time was q^2-dependent indicating that the relaxation was caused by cooperative diffusion of the solute. The apparent diffusion coefficient D was calculated from the average relaxation rate of this relaxation mode as $D=\langle\tau^{-1}\rangle/q^2$. D is related to the apparent hydrodynamic radius, R_a, of the solute according to equation 2.

$$R_a = \frac{kT}{6\pi\eta D} \qquad \text{equation 2}$$

with k Boltzmann's constant, T the absolute temperature and η the viscosity of the solvent. When the particles are small compared to q^{-1} and the solutions are sufficiently dilute so that interactions can be neglected R_a is equal to the z-average hydrodynamic radius, R_h.

Static Light Scattering (SLS). The Rayleigh ratio, R_θ, of the solution was determined following equation 3.

$$R_\theta = \frac{I_{solution}(\theta) - I_{solvent}(\theta)}{I_{toluene}(\theta)} \cdot \left(\frac{n_{solvent}}{n_{toluene}} \right)^2 . R_{toluene} \qquad \text{equation 3}$$

with $I_{solution}$, $I_{solvent}$, $I_{toluene}$ the average intensities scattered respectively by the solution, the solvent and the reference (toluene), $n_{solvent}$ = 1.426 (cyclohexane) and $n_{toluene}$ = 1.496 the respective refractive indexes of the solvent and of toluene and $R_{toluene} = 1.35 \times 10^{-5}$ cm^{-1} the Rayleigh ratio of toluene for a wavelength λ = 632.8 nm.

At a given concentration C, R_θ is related to the apparent weight average molecular weight of the scatterers, M_a, and to the q-dependent structure factor, S(q), see equations 4 and 5.[42] Note that M_a corresponds to the true molecular weight, M_w, only in very dilute solutions where the interactions between the scatterers can be neglected. At higher concentration, interactions cause M_a to differ strongly from M_w.[42]

$R_\theta = K.C.M_a.S(q)$ equation 4

with C the polymer concentration in g/L and K a constant:

$$K = \frac{4\pi^2 n_{solvent}^2}{\lambda^4 N_a} \left(\frac{\partial n}{\partial C} \right)^2 \qquad \text{equation 5}$$

where N_a is Avogadro's number.

For $S_{14}U_3S_{14}$ the scatterers were small, so that $q.R_g < 1$, R_g being their apparent radius of gyration. In this case, equation 4 may be approximated to equation 6 corresponding to the Zimm approximation, so that R_g could be calculated.[42] R_g of $S_{34}U_3S_{34}$ was close to the lower resolution limit of light scattering so that the value of R_g is only a rough estimate in this case. Representative plots are shown for $S_{14}U_3S_{14}$ and $S_{34}U_3S_{34}$ in Figure S9 of the Supporting Information.

$$\frac{KC}{R_\theta} = \frac{1}{M_a.S(q)} = \frac{1}{M_a}.\left(1 + \frac{q^2.R_g^2}{3}\right) \qquad \text{equation 6}$$

When the solutions were cooled, the polymers became insoluble at a characteristic precipitation temperature noted T_p. Precipitation was characterized by a sharp increase of the scattered light intensity and T_p is therefore also called the cloud point and could be determined by light scattering at a scattering angle of 90°. The cells were immersed in a decalin bath controlled to ± 0.1°C and in the vicinity of the cloud point the temperature of the bath was lowered in steps of 1°C. After each step sufficient time was allowed for the solution to reach steady-state. The precipitation temperature was detected with an accuracy of ± 1°C.

Small Angle Neutron Scattering (SANS).

Measurements were made at the LLB (Saclay, France) on the Pace instrument, at two distance-wavelength combinations to cover the 4.10^{-3} to 0.2 $Å^{-1}$ q-range, where the scattering vector q is defined as usual, assuming elastic scattering, as $q=(4\pi/\lambda)\sin(\theta/2)$, where θ is the angle between incident and scattered beam. Data were corrected for the empty cell signal and the solute and solvent incoherent background. A light water standard was used to normalize the scattered intensities to cm^{-1} units.

The measurements were done at a polymer concentration c ~ 15 g/L and at 21 ± 2°C.

Differential Refractometry. Measurements were performed on an OptiLab rEX from Wyatt Technology Corporation (λ_0=632nm). The refractive index was measured in cyclohexane at various concentrations of $S_{14}U_3S_{14}$ and $S_{34}U_3S_{34}$ ranging from 1 to 5 g/L. In cyclohexane, for $S_{14}U_3S_{14}$ and $S_{34}U_3S_{34}$ $\partial n/\partial c = 0.18$ mL.g^{-1} , which is in agreement with the value found in the literature for PS in this solvent.[43]

Results and discussion

1. Synthesis of the PS-functional trisureas $S_{14}U_3S_{14}$ and $S_{34}U_3S_{34}$

Two trisureas functionalized symmetrically by two PS side-arms were obtained in five straightforward steps (Figure 1) as described in detail in Supporting Information. Briefly, the first three steps consisted in the synthesis of monodisperse amino-functional PS of the desired lengths by Atom Transfer Radical Polymerization (ATRP) according to procedures adapted from the literature[44, 45], see Figure 1a-c. In a fourth parallel step, 2,4-TDI was dimerized by reaction with water in ether following a procedure published elsewhere[38, 46] (Figure 1d), yielding T_0. The targeted trisureas $S_{14}U_3S_{14}$ and $S_{34}U_3S_{34}$, whose PS arms are monodisperse and have number-average degrees of polymerization of 14 and 34 respectively, were finally obtained by reacting an excess of the amino-functional polystyrene (S_{14}-NH_2 or S_{34}-NH_2 respectively) with T_0 (Figure 1e).

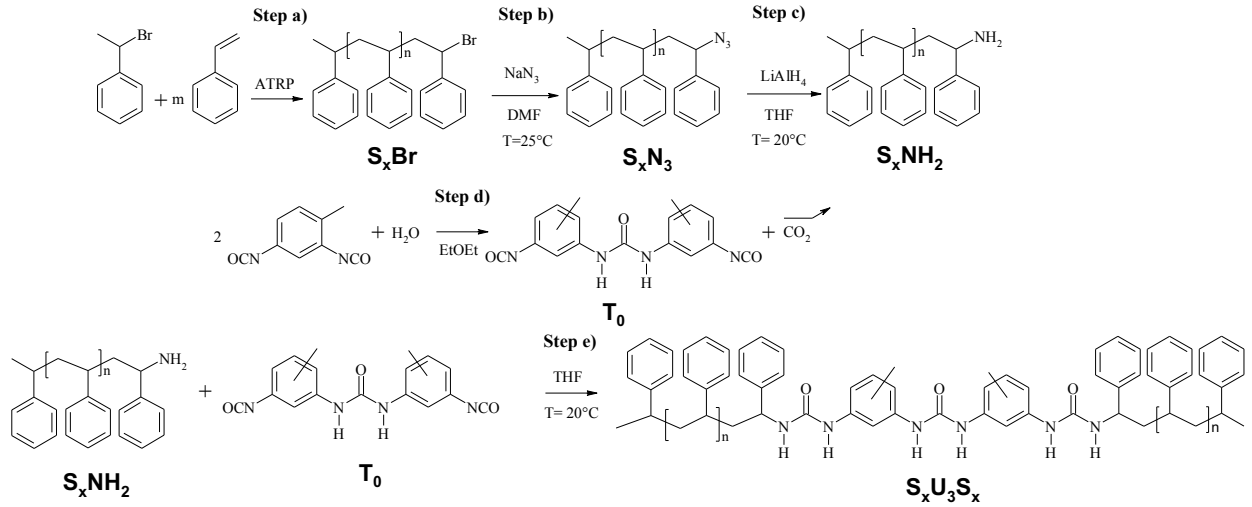

Figure 1. Five steps synthesis of two trisureas, $S_{14}U_3S_{14}$ and $S_{34}U_3S_{34}$, functionalized by PS side-arms having number average degrees of polymerization x = n+2 = 14 or 34 respectively.

2. Self assembly in cyclohexane.

Self-assembly at 50°C. Cyclohexane is a Θ solvent for linear polystyrene at 34.5°C.[41] The self-assembly of $S_{14}U_3S_{14}$ and of $S_{34}U_3S_{34}$ was therefore first studied at 50°C, i.e. in conditions where cyclohexane is a moderate solvent of the PS arms so that the self-assembly is not perturbed by solvophobic interactions and is only driven by hydrogen bonds. The influence of the concentration on the self-assembly of $S_{14}U_3S_{14}$ and $S_{34}U_3S_{34}$ was investigated over a broad concentration range (0.12–115 g/L for $S_{14}U_3S_{14}$ and 0.5–100 g/L for $S_{34}U_3S_{34}$). At lower concentrations the scattering intensity was too low to allow accurate measurements.

The concentration dependence of the apparent molar mass follows the same trend for $S_{14}U_3S_{14}$ and $S_{34}U_3S_{34}$, see Figure 2. M_a, first increases very slightly with increasing concentration and decreases strongly at higher concentration. M_a is always higher than the molecular weight of single $S_{14}U_3S_{14}$ or $S_{34}U_3S_{34}$ molecules, indicating that self-assembly does occur in both cases. The slight increase of

M_a with the polymer concentration in the low concentration regime may either be the result of attractive interactions between scatterers of constant size or of an increase of M_w with increasing concentration. Below we will show that solvophobic interactions can be neglected at 50°C in cyclohexane. Therefore the weak initial increase of M_a is probably caused by weak growth of the aggregates with increasing concentration. However, the increase of M_a up to 10 g/L is much weaker than the growth predicted for an open association scenario: $M_w \propto C^{\alpha}$ with $\alpha \geq 0.5$[47, 48] and can be neglected in first approximation. The decrease of M_a at higher polymer concentration is due to repulsive, excluded volume, interactions between the aggregates.

$S_{14}U_3S_{14}$ self-assembles into much larger aggregates than $S_{34}U_3S_{34}$. Indeed, the molecular weight of the aggregates formed by $S_{34}U_3S_{34}$ determined in the dilute regime ($C < 20$ g/L) was $M_w \approx 4.8 \times 10^4$ g/mol, corresponding to an aggregation number $N_{agg} = M_w(\text{aggregates})/M_w(S_{34}U_3S_{34}) \approx 5.5$ with $M_w(S_{34}U_3S_{34}) = 8500$ g/mol the molecular weight of the unimers. Considering that the distance between two hydrogen bonded urea groups is 0.46 nm,[49] the corresponding weight-average length of the supramolecular backbone is $0.46 \times (N_{agg}-1) \sim 2$ nm. For the aggregates formed by $S_{14}U_3S_{14}$ we found $M_w \approx 4.0 \times 10^5$ g/mol, corresponding to $N_{agg} \approx 100$ and a total length of the supramolecular backbone of about 50 nm. Moreover, the radius of gyration of the aggregates was $R_g = 15 \pm 2$ nm for $S_{34}U_3S_{34}$ and $R_g = 24 \pm 2$ nm for $S_{14}U_3S_{14}$. For both systems R_g was independent of the polymer concentration within the experimental error. The larger size of aggregates of $S_{14}U_3S_{14}$ explains why the decrease of M_a with increasing concentration started at a lower concentration (10 g/L) for $S_{14}U_3S_{14}$ than for $S_{34}U_3S_{34}$ (20 g/L).

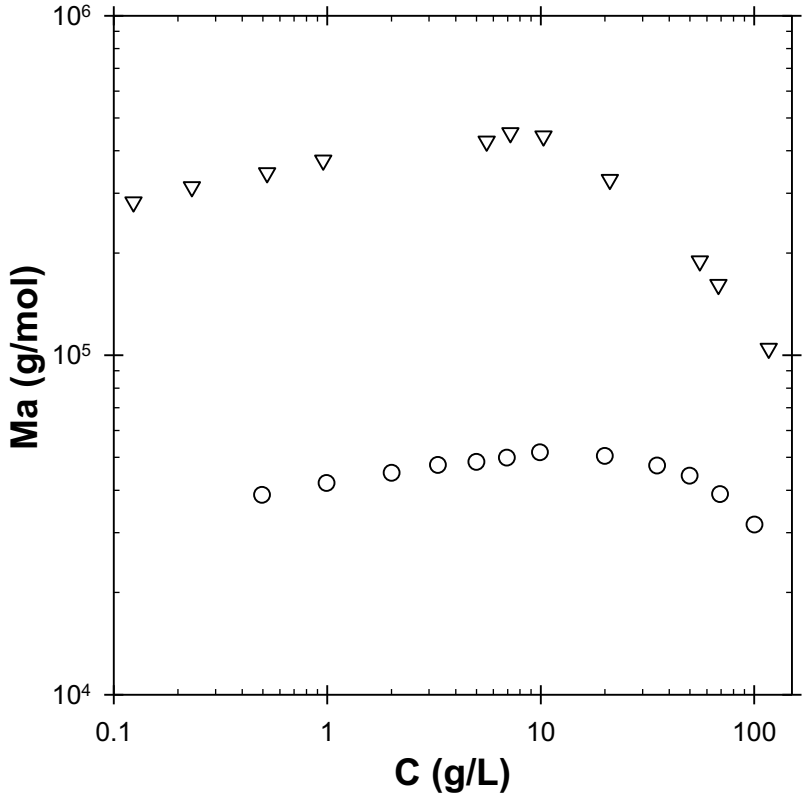

Figure 2. Evolution of the apparent molar mass M_a of $S_{34}U_3S_{34}$ (○) and $S_{14}U_3S_{14}$ (▽) as a function of the polymer concentration obtained by light scattering at 50°C in cyclohexane.

Only one, relatively broad, diffusive relaxation mode was observed for all solutions by dynamic light scattering (DLS), see Figure S10 of the Supporting Information. The apparent hydrodynamic radius, R_a, is plotted as a function of the concentration in Figure 3. R_a of aggregates formed by $S_{34}U_3S_{34}$ increased very weakly between 1 and 20 g/L and somewhat stronger at higher concentrations. The latter may indicate growth of the aggregates, but one also needs to consider that, contrary to M_a, the cooperative diffusion is influenced by an increase of the friction coefficient with increasing concentration which may cause an increase of R_a.[42] The hydrodynamic radius of aggregates of $S_{34}U_3S_{34}$ determined at low concentrations ($R_h \approx 5$ nm), was much larger than the

backbone length (2 nm), which means that the small aggregates formed by $S_{34}U_3S_{34}$ are not very anisotropic, but more akin to star polymers. The hydrodynamic radius of $S_{14}U_3S_{14}$ increased with increasing concentration from 10 to 15 nm between 0.2 and 10 g/L. These values are significantly smaller than the calculated backbone length (50 nm) implying that the larger aggregates formed by $S_{14}U_3S_{14}$ are rod-like.

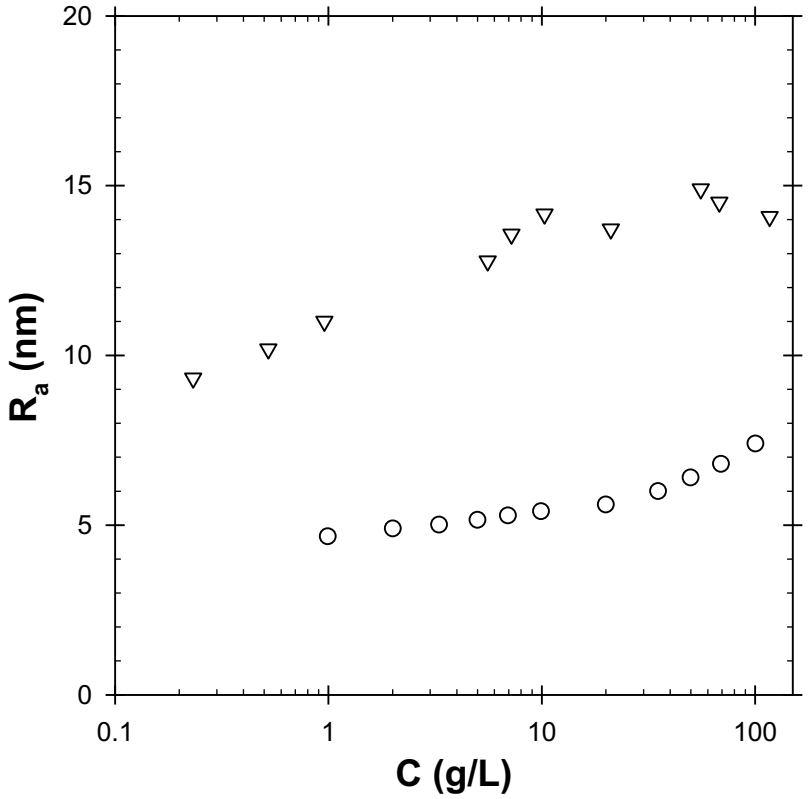

Figure 3. Evolution of the apparent hydrodynamic radius R_a of $S_{34}U_3S_{34}$ (○) and $S_{14}U_3S_{14}$ (▽) as a function of the polymer concentration obtained by dynamic light scattering at 50°C in cyclohexane.

The rod-like morphology of $S_{14}U_3S_{14}$ aggregates was confirmed by Small Angle Neutron Scattering (SANS) in deuterated cyclohexane, see Figure 4. Indeed, a q^{-1}-dependence of the scattered

intensity, expected for rods, was observed from 4.10^{-3} Å^{-1} to ~ 4.10^{-2} Å^{-1}. Interestingly, a q^{-2} dependence of the scattered intensity, characteristic of gaussian chains, is observed at the highest q values. The combination of the low-q rod-like character and high-q flexible chain character suggests the presence of hairy rod-like objects. Therefore, a fit of the data was attempted with the form factor of a simple cylinder,[50] but also with the form factor of a hairy rod-like micelle (see Supporting Information).[51] Both models yield a reasonably good fit at low and intermediate q values, with parameter values that are compatible with the formation of a rod-like core composed of hydrogen bonded ureas. The fact that the agreement at high-q is not perfect is probably due to the specific shape of the core cross-section.

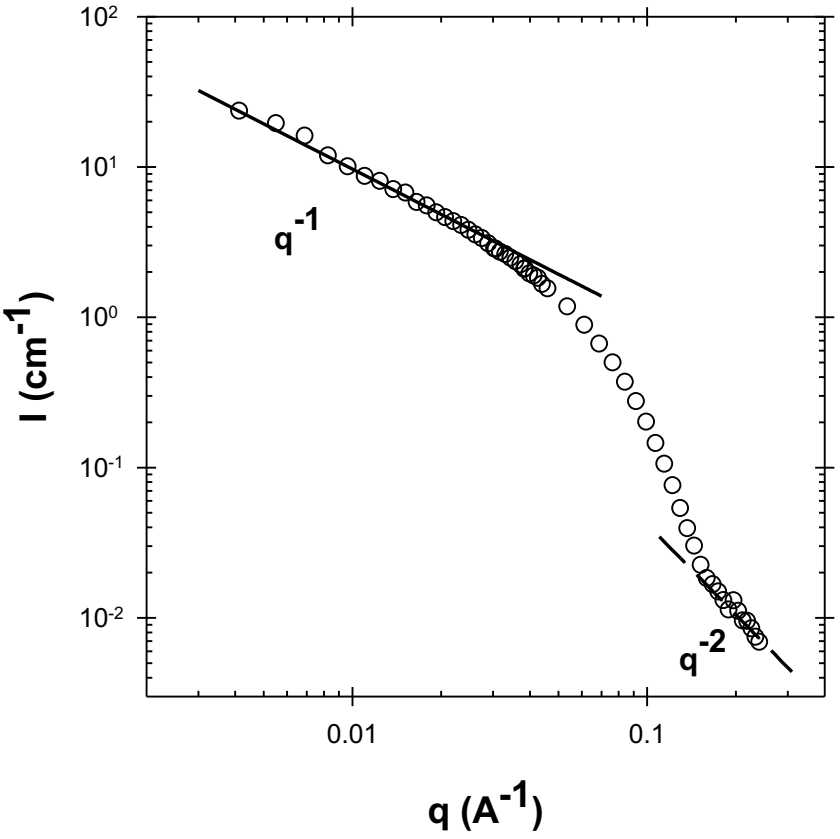

Figure 4. SANS intensity (I) versus scattering vector (q) for solutions of $S_{14}U_3S_{14}$ (○) in d_{12}-cyclohexane at 16 g/L and 21°C. The straight lines indicate q^{-1} (continuous) and q^{-2} (dashed) dependencies.

To summarize, $S_{34}U_3S_{34}$ forms small aggregates which correspond to supramolecular star-shaped PS with a small number of arms. Larger aggregates which are significantly anisotropic can be obtained with $S_{14}U_3S_{14}$ by reducing the size of the PS arms, resulting in average-sized supramolecular bottle-brushes. The self-assembly of both molecules is however much weaker than that of U3PIB2, a trisurea decorated with two polyisobutylene (PIB) arms with $DP_n = 27$. The latter is indeed able to form bottle brushes with aggregation numbers higher than 600 (persistence length > 300 nm) in the same solvent[38]. These results thus point out the dramatic effect of both the chemical nature and the degree of polymerization of the polymer side-chains on the self-assembly of trisurea-based molecules.

Two aspects must probably be taken into account to understand these results. First, as already pointed out,[38] a theoretical model by Wang et al.[52] indicates that the side-arms must stretch to accommodate within a bottle-brush morphology. This results in a conformational entropic penalty which must be compensated by strong enough hydrogen bonds between the self-assembling units if long bottle-brushes are to be formed. Clearly, the conformational entropic loss increases when the degree of polymerization of the PS side-chains increases, which explains why $S_{34}U_3S_{34}$ forms much smaller bottle brushes than $S_{14}U_3S_{14}$. Considering how large the effect is, very short PS arms are required to obtain long anisotropic PS bottle-brushes. Second, even $S_{14}U_3S_{14}$ whose side-arms have a smaller DP_n than U3PIB2 forms much shorter bottle brushes than the latter. This observation can obviously not be explained by the number of monomer units in the side-arms. It is neither

related to the difference of polarity of the side-arms as both types of arms are non polar and therefore hardly compete with the formation of hydrogen bonds. The observed differences must therefore be related to the steric hindrance of the monomer units close to the trisurea functions. According to the bulk density of the polymers and the molecular weight of their monomer units, the volume occupied by styrene units in the bulk (V_S = 0.17 nm^3/unit) is almost twice as large as that of isobutylene units (V_{IB} = 0.10 nm^3/unit), hinting at much more bulky S than IB units. As a consequence, the first few styrene units connected to the trisurea functions probably hinder much more the formation of hydrogen bonds than the isobutylene units because of their bulkiness. It has indeed been observed that monoureas self-assemble much more weakly when they are substituted by very bulky alkyl chains.[53] The negative effect of the styrene units may be amplified by the fact that they are directly connected to the trisurea functions without any spacer, see Figure 1. Adding an *n*-alkyl spacer between the trisurea function and the first styrene units may help to decrease this effect and obtain longer PS bottle brushes.

Our results contrast strongly with those obtained for cyclic oligopeptides. Indeed, Couet et al.[22] reported that the length of supramolecular assemblies of cyclic oligopeptides was exclusively controlled by the degree of polymerization of the side-chains and did not vary significantly when poly(*n*-butyl acrylate) (P*n*BA) side-chains were replaced by poly(N-isopropyl acrylamide) (PNIPAM) or by much bulkier PS side-chains of the same degree of polymerization. Moreover, the general trend observed by Chapman et al.[27] was that the total length of nanotubes formed by cyclic oligopeptides decorated by two P*n*BA arms did vary as a function of the degree of polymerization of the arms, but only moderately. The difference observed between trisureas-based and cyclic-oligopeptide-based bottle-brushes may be due to a significant difference in the packing density. Indeed, in the case of the trisurea core, the distance between two adjacent arms is fixed by

the urea hydrogen bond (ca 4.6Å), whereas in the case of the cyclic-oligopeptide core, the distance between two adjacent arms can be increased by rotation of one cyclic peptide with respect to its neighbor. If this is the case, both the effect of the steric hindrance of the first monomer units and the necessity for the chains to stretch would be strongly diminished. It must also be mentioned that six hydrogen bonds per self-assembling units are formed for trisureas, whereas height are formed for cyclic oligopeptides. The increased number of hydrogen bonds in the latter case may render the self-assembly of cyclic oligopeptides less sensitive to the effect of the side arms.

Effect of the temperature. PS exhibits a critical solubility temperature, T_c, in cyclohexane which has been predicted theoretically to depend on the topology (linear, star-like, bottle-brush) of the chain.[54-57] A reduction of T_c has been predicted for more branched structures compared to linear PS of the same molecular weight due to the fact that less interaction between segments of different molecules can develop when they are close to the branch points.

For $S_{34}U_3S_{34}$ which forms star-like aggregates with a small number of arms (N_{agg} ~ 5.5 corresponding to ~ 11 arms), the critical temperature T_c was only slightly lower than that of a linear polystyrene of the same molecular weight as that of $S_{34}U_3S_{34}$ aggregates. This result confirms both the theory and previous experimental evidences reporting only a very small reduction of T_c (by 2-3°C) for star-shaped polystyrenes with a relatively small number of arms (< 12),[41,58-63] Moreover, the temperature hardly affected the self-assembly of $S_{34}U_3S_{34}$: N_{agg} remained almost constant until precipitation occurred. Details are given in Figure S12 of the Supporting Information for this polymer.

$S_{14}U_3S_{14}$ was much more interesting because it forms bottle-brush PS with a large number of arms (N_{agg} ~ 100, corresponding to ~ 200 arms) whose critical temperature had never been compared

experimentally to that of linear PS of the same molecular weight. The concentration dependence of M_a at different temperatures is shown in Figure 5 for $S_{14}U_3S_{14}$. At all temperatures, M_a increased initially weakly with increasing concentration and was considered to be equal to M_w at low concentration. M_w increased moderately with decreasing temperature from about 2.5 10^5 g/mol (N_{agg} = 65) at 60°C to about 5.0 10^5 g/mol (N_{agg}= 130) at 14°C. The influence of the temperature on M_w may be partly explained by the fact that at lower temperatures the effective excluded volume interaction between the PS segments is reduced as was suggested by Dingenouts et al.[12] and the arms hinders less the self-assembly. However, an increase of the strength of the hydrogen bonds at lower temperature can also play a role. For T>20°C, the evolution of M_a with polymer concentration was qualitatively similar to what was observed at 50 °C. However, for T ≤ 20°C, M_a increased more strongly with the concentration above about 5 g/L before decreasing at the highest concentrations. The effect amplified with decreasing temperature until at 14 °C precipitation was observed. These phenomena were caused by the increase of attractive interactions between the aggregates due to the decrease of the solvent quality for PS. At all temperatures above 14°C and at high concentrations, M_a decreased with increasing concentration, because repulsive excluded volume interactions dominated.

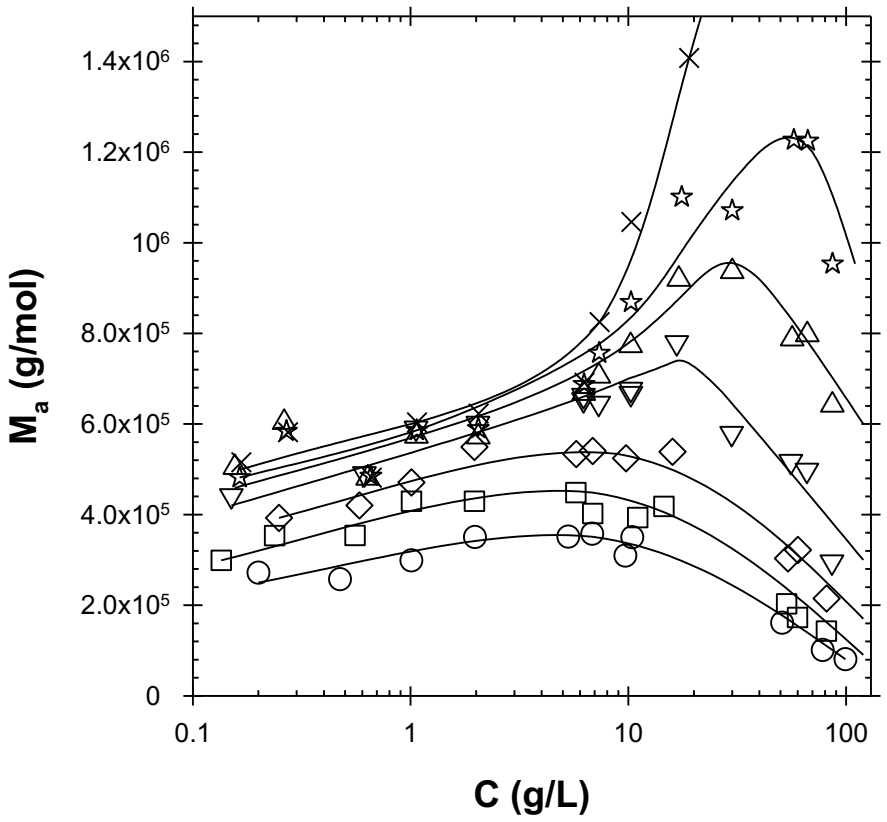

Figure 5. Evolution of the apparent molar mass of $S_{14}U_3S_{14}$ as a function of the concentration at 60°C (○), 40°C (□), 25°C (◇), 20°C (▽), 18°C (△), 16°C (☆) and 14°C (×) measured at an angle of 90°. The lines are guides to the eyes.

The cloud point temperature of $S_{14}U_3S_{14}$ was determined at different concentrations and is plotted as a function of the volume fraction (ϕ) in Figure 6 ($\phi = C/\rho$, with ρ = 930 g/L the density of polystyrene in cyclohexane). The critical temperature, T_c = 15°C, corresponds to the highest cloud-point temperature T_p as a function of ϕ. The behavior of the bottle-brush polymers are compared with that of a linear PS ($M_w = 2.0\ 10^5$ g/mol)[64] and of a 4–arms star ($M_w = 1.6\ 10^5$ g/mol)[41] with somewhat lower molar masses than the $S_{14}U_3S_{14}$ bottle brushes. We note that the critical

temperature decreases with decreasing molecular weight for linear PS.[64, 65] Both the linear (T_c = 24°C) and the star (T_c = 21°C) polymers phase separated at significantly higher temperatures than the bottle brush $S_{14}U_3S_{14}$ (T_c = 15 °C) even though their molar masses were lower. The effect cannot be attributed to the trisurea forming the backbone of $S_{14}U_3S_{14}$ bottle brushes, as a trisurea decorated with short solvophilic 2-ethylhexyl side-chains was not soluble in cyclohexane.[38]

It can therefore be concluded that, in cyclohexane, a bottle-brush architecture leads to a much larger decrease of T_c with respect to a linear PS of the same molecular weight than a star architecture. Our results confirm experimentally for the first time the theories about the effect of a bottle brush architecture on T_c. The observed reduction of T_c was similar to that reported for star PS with short arms in methyl cyclohexane, a solvent in which architecture effects are much more significant than in cyclohexane.[66]

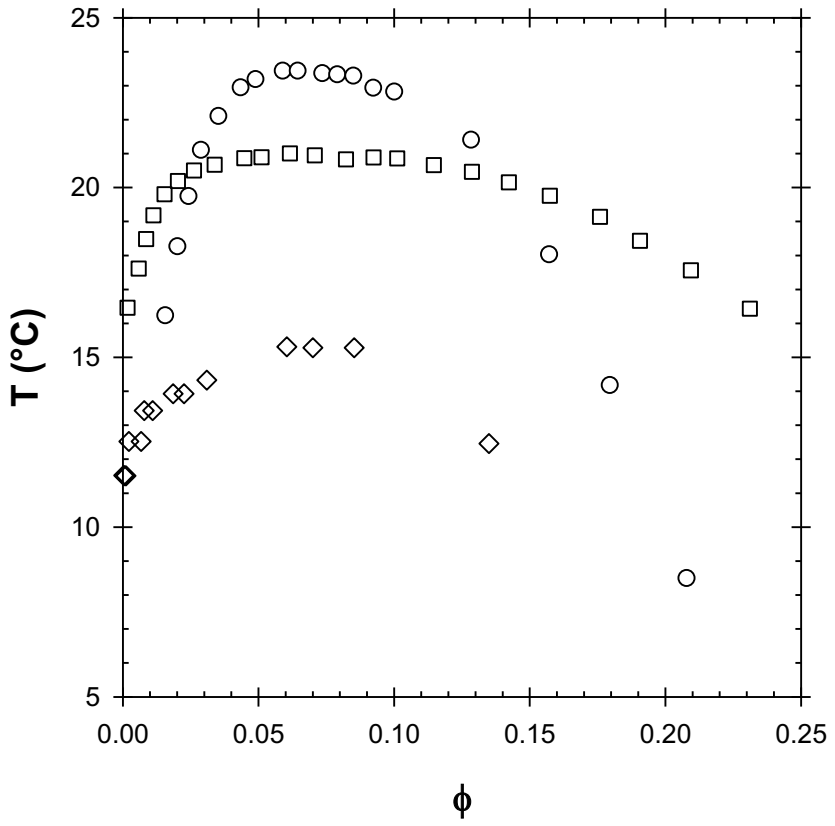

Figure 6. Precipitation temperatures (= cloud point) T_p for (○) linear PS (M_w = 200000 g/mol, adapted from ref[64]), (□) four armed star PS (M_w = 155000 g/mol, adapted from ref[41]) and (◇) bottle-brush supramolecular PS ($S_{14}U_3S_{14}$, M_w = 400000 g/mol, N_{agg} = 100, this work) in cyclohexane as a function of the polymer volume fractions.

Conclusion

Trisureas, consisting of three urea units separated by rigid aromatic rings, were functionalized by poly(styrene) side-chains following a straightforward synthesis involving the preparation of amino-functional PS by Atom Transfer Radical Polymerization and their coupling to the trisurea units. Two different number average degrees of polymerization of the PS arms were prepared (DP_n

= 14 for $S_{14}U_3S_{14}$ and DP_n = 34 for $S_{34}U_3S_{34}$), but the proposed synthetic route allows a variation of the size of the PS arms in a controlled manner.

Both $S_{34}U_3S_{34}$ and $S_{14}U_3S_{14}$ self-assembled via hydrogen bonding of the trisurea units leading to nano-sized aggregates. However, the number of aggregation of the latter was about 20 times as high as that of the former and both polymers assembled into much smaller aggregates than a trisurea decorated by two PIB side-chains with a similar degree of polymerization. This revealed that the self-assembly of trisureas is strongly influenced both by the chemical nature and degree of polymerization of the side-chains in strong contrast to what was observed for polymer-decorated cyclic oligopeptides for which the effect was rather weak.

$S_{14}U_3S_{14}$ did however form truly anisotropic bottle brushes and could be used as a model to study the impact of the architecture of PS on its critical solubility temperature (T_c) in cyclohexane. For the first time, it was shown that T_c is much lower for a bottle-brush PS than for a linear PS of similar molecular weight. The effect is much more pronounced than has been reported for star-like PS in cyclohexane.

ASSOCIATED CONTENT

Supporting Information. 1) Synthesis of $S_{14}U_3S_{14}$ and $S_{34}U_3S_{34}$ including the experimental details, the kinetic monitoring of the ATRP polymerization of S_{14}-Br and S_{34}-Br and the quantitative functionalization of S-Br into S-N_3 and S-NH_2. 2) Characterization of the self-assembly in cyclohexane by light scattering: determination of R_g, R_h distributions. 3) Characterization of the self-assembly of $S_{14}U_3S_{14}$ in cyclohexane by small angle neutron scattering – form factor for a simple cylinder and for a hairy rod-like micelle. 4) Determination of the cloud point T_p of $S_{34}U_3S_{34}$ in

cyclohexane at different concentrations. This material is available free of charge via the Internet at http://pubs.acs.org.

AUTHOR INFORMATION

Corresponding Authors

email: olivier.colombani@univ-lemans.fr

Tel: +33 2 43 83 33 15 / Fax: +33 2 43 83 35 58

Author Contributions

The manuscript was written through contributions of all authors. All authors have given approval to the final version of the manuscript.

Funding Sources

This work has been funded by the Agence Nationale de la Recherche in the frameworks ANR-2011-JS08-006-01 and ANR-10-BLAN-0801.

ACKNOWLEDGMENT

The authors thank Christophe Chassenieux, Amélie Durand and Emmanuelle Mebold for their help respectively with the SEC, NMR and MALDI TOF MS analyses, and A. Lange and BASF company for the gift of a Kerocom PIBA sample.

REFERENCES

1. Scanlon, S.; Aggeli, A. *Nano Today* **2008,** 3, (3–4), 22-30.

2. Park, T.; Zimmerman, S. C. *J. Am. Chem. Soc.* **2006,** 128, (43), 13986-13987.

3. Corbin, P. S.; Lawless, L. J.; Li, Z.; Ma, Y.; Witmer, M. J.; Zimmerman, S. C. *Proc. Natl. Acad. Sci. U.S.A.* **2002,** 99, (8), 5099-5104.

4. Percec, V.; Dulcey, A. E.; Balagurusamy, V. S. K.; Miura, Y.; Smidrkal, J.; Peterca, M.; Nummelin, S.; Edlund, U.; Hudson, S. D.; Heiney, P. A.; Duan, H.; Magonov, S. N.; Vinogradov, S. A. *Nature* **2004,** 430, (7001), 764-768.

5. Katsuhiko, A.; Jonathan, P. H.; Michael, V. L.; Ajayan, V.; Richard, C.; Somobrata, A. *Sci. Technol. Adv. Mater.* **2008,** 9, (1), 014109.

6. Zhang, M.; Müller, A. H. E. *J. Polym. Sci., Part A: Polym. Chem.* **2005,** 43, 3461–3481.

7. Sheiko, S. S.; Sumerlin, B. S.; Matyjaszewski, K. *Prog. Polym. Sci.* **2008,** 33, 759– 785.

8. Feng, C.; Li, Y.; Yang, D.; Hu, J.; Zhang, X.; Huang, X. *Chem. Soc. Rev.* **2011,** 40, 1282–1295.

9. Brinke, G. T.; Ikkala, O. *Chem. Rec.* **2004,** 4, (4), 219-230.

10. Weck, M. *Polym. Int.* **2007,** 56, (4), 453-460.

11. Chapman, R.; Danial, M.; Koh, M. L.; Jolliffe, K. A.; Perrier, S. *Chem. Soc. Rev.* **2012,** 41, (18), 6023-6041.

12. Dingenouts, N.; Klyatskaya, S.; Rosenfeldt, S.; Ballauff, M.; Höger, S. *Macromolecules* **2009,** 42, (15), 5900-5902.

13. Fritzsche, M.; Jester, S.-S.; Höger, S.; Klaus, C.; Dingenouts, N.; Linder, P.; Drechsler, M.; Rosenfeldt, S. *Macromolecules* **2010,** 43, (20), 8379-8388.

14. Höger, S. *Chem.–Eur. J.* **2004,** 10, (6), 1320-1329.

15. Höger, S.; Bonrad, K.; Rosselli, S.; Ramminger, A.-D.; Wagner, T.; Silier, B.; Wiegand, S.; Häußler, W.; Lieser, G.; Scheumann, V. *Macromol. Symp.* **2002,** 177, (1), 185-191.

16. Rosselli, S.; Ramminger, A.-D.; Wagner, T.; Lieser, G.; Höger, S. *Chem.–Eur. J.* **2003,** 9, (15), 3481-3491.

17. Rosselli, S.; Ramminger, A.-D.; Wagner, T.; Silier, B.; Wiegand, S.; Häußler, W.; Lieser, G.; Scheumann, V.; Höger, S. *Angew. Chem. Int. Ed.* **2001,** 40, (17), 3137-3141.

18. Byrne, N.; Menzies, D.; Goujon, N.; Forsyth, M. *Chem. Commun.* **2013,** 49, (70), 7729-7731.

19. Couet, J.; Samuel, J. D. J. S.; Kopyshev, A.; Santer, S.; Biesalski, M. *Angew. Chem. Int. Ed.* **2005,** 44, (21), 3297-3301.

20. Couet, J.; Biesalski, M. *Macromolecules* **2006,** 39, (21), 7258-7268.

21. Couet, J.; Biesalski, M. *Soft Matter* **2006,** 2, (12), 1005-1014.

22. Couet, J.; Biesalski, M. *Small* **2008,** 4, (7), 1008-1016.

23. Loschonsky, S.; Couet, J.; Biesalski, M. *Macromol. Rapid Commun.* **2008,** 29, (4), 309-315.

24. Chapman, R.; Jolliffe, K. A.; Perrier, S. *Aust. J. Chem.* **2010,** 63, (8), 1169-1172.

25. Chapman, R.; Jolliffe, K. A.; Perrier, S. *Polym. Chem.* **2011,** 2, (9), 1956-1963.

26. Chapman, R.; Jolliffe, K. A.; Perrier, S. *Adv. Mater.* **2013,** 25, (8), 1170-1172.

27. Chapman, R.; Koh, M. L.; Warr, G. G.; Jolliffe, K. A.; Perrier, S. *Chemical Science* **2013,** 4, (6), 2581-2589.

28. Chapman, R.; Warr, G. G.; Perrier, S.; Jolliffe, K. A. *Chem.–Eur. J.* **2013,** 19, (6), 1955-1961.

29. Chapman, R.; Bouten, P. J. M.; Hoogenboom, R.; Jolliffe, K. A.; Perrier, S. *Chem. Commun.* **2013,** 49, (58), 6522-6524.

30. ten Cate, M. G. J.; Severin, N.; Börner, H. G. *Macromolecules* **2006,** 39, (23), 7831-7838.

31. Balbo Block, M. A.; Hecht, S. *Angew. Chem. Int. Ed.* **2005,** 44, (43), 6986-6989.

32. Danial, M.; Tran, C. M. N.; Jolliffe, K. A.; Perrier, S. *J. Am. Chem. Soc.* **2014,** 136, (22), 8018-8026.

33. Hentschel, J.; ten Cate, M. G. J.; Börner, H. G. *Macromolecules* **2007,** 40, (26), 9224-9232.

34. Hourani, R.; Zhang, C.; van der Weegen, R.; Ruiz, L.; Li, C.; Keten, S.; Helms, B. A.; Xu, T. *J. Am. Chem. Soc.* **2011,** 133, (39), 15296-15299.

35. Ruiz, L.; Keten, S. *Soft Matter* **2014,** 10, (6), 851-861.

36. Tian, L.; Szilluweit, R.; Marty, R.; Bertschi, L.; Zerson, M.; Spitzner, E.-C.; Magerled, R.; Frauenrath, H. *Chem. Sci.* **2012,** 3, 1512–1521.

37. Pensec, S.; Nouvel, N.; Guilleman, A.; Creton, C.; Boué, F.; Bouteiller, L. *Macromolecules* **2010,** 43, (5), 2529-2534.

38. Catrouillet, S.; Fonteneau, C.; Bouteiller, L.; Delorme, N.; Nicol, E.; Nicolai, T.; Pensec, S.; Colombani, O. *Macromolecules* **2013,** 46, (19), 7911-7919.

39. Fonteneau, C.; Pensec, S.; Bouteiller, L. *Polym. Chem.* **2014,** 5, (7), 2496-2505.

40. Danial, M.; My-Nhi Tran, C.; Young, P. G.; Perrier, S.; Jolliffe, K. A. *Nat Commun* **2013,** 4.

41. Terao, K.; Okumoto, M.; Nakamura, Y.; Norisuye, T.; Teramoto, A. *Macromolecules* **1998,** 31, (20), 6885-6890.

42. Brown, W., *Light Scattering: Principles and Development*. Clarendon Press: Oxford, U.K.: Oxford, 1996.

43. Huglin, M. B., *Light Scattering from Polymer Solutions*. Academic Press: London, New York, 1972.

44. Matyjaszewski, K.; Nakagawa, Y.; Gaynor, S. G. *Macromol. Rapid Commun.* **1997,** 18, (12), 1057-1066.

45. Coessens, V.; Pintauer, T.; Matyjaszewski, K. *Prog. Polym. Sci.* **2001,** 26, (3), 337-377.

46. Pelley, R. L. *Process for the Preparation of Substituted Di(isocyanatophenyl) Ureas*. U.S. Patent 2,757,184, July 31, 1956.

47. Lortie, F.; Boileau, S.; Bouteiller, L.; Chassenieux, C.; Lauprêtre, F. *Macromolecules* **2005,** 38, (12), 5283-5287.

48. Zhao, D.; Moore, J. S. *Org. Biomol. Chem.* **2003,** 1, (20), 3471-3491.

49. Pérez-Folch, J.; Subirana, J. A.; Aymami, J. *J. Chem. Crystallogr.* **1997,** 27, (6), 367-369.

50. Terech, P.; Coutin, A. *Langmuir* **1999,** 15, (17), 5513-5525.

51. Pedersen, J. *J. Appl. Crystallogr.* **2000,** 33, (3 Part 1), 637-640.

52. Wang, Z. G.; Safran, S. A. *J. Chem. Phys.* **1988,** 89, (8), 5323-5328.

53. Lortie, F.; Boileau, S.; Bouteiller, L. *Chem.–Eur. J.* **2003,** 9, (13), 3008-3014.

54. Candau, F.; Rempp, P.; Benoit, H. *Macromolecules* **1972,** 5, (5), 627-635.

55. Enders, S.; Langenbach, K.; Schrader, P.; Zeiner, T. *Polymers* **2012,** 4, (1), 72-115.

56. Yang, J.; Peng, C.; Liu, H.; Hu, Y.; Jiang, J. *Fluid Phase Equilib.* **2006,** 244, (2), 188-192.

57. Arya, G.; Panagiotopoulos, A. Z. *Macromolecules* **2005,** 38, (25), 10596-10604.

58. Cowie, J. M. G.; Horta, A.; McEwen, I. J.; Prochazka, K. *Polym. Bull.* **1979,** 1, (5), 329-335.

59. Okumoto, M.; Terao, K.; Nakamura, Y.; Norisuye, T.; Teramoto, A. *Macromolecules* **1997,** 30, (24), 7493-7499.

60. Okumoto, M.; Tasaka, Y.; Nakamura, Y.; Norisuye, T. *Macromolecules* **1999,** 32, (22), 7430-7436.

61. Tasaka, Y.; Okumoto, M.; Nakamura, Y.; Norisuye, T. *Polym. J* **2008,** 40, (7), 634-639.

62. Orofino, T. A.; Wenger, F. *J. Phys. Chem.* **1963,** 67, (3), 566-575.

63. Yokoyama, H.; Takano, A.; Okada, M.; Nose, T. *Polymer* **1991,** 32, (17), 3218-3224.

64. Kuwahara, N.; Nakata, M.; Kaneko, M. *Polymer* **1973,** 14, (9), 415-419.

65. Saeki, S.; Kuwahara, N.; Konno, S.; Kaneko, M. *Macromolecules* **1973,** 6, (2), 246-250.

66. Alessi, M. L.; Bittner, K. C.; Greer, S. C. *J. Polym. Sci., Part B: Polym. Phys*. **2004,** 42, (1), 129-145.

FOR TABLE OF CONTENT USE ONLY.

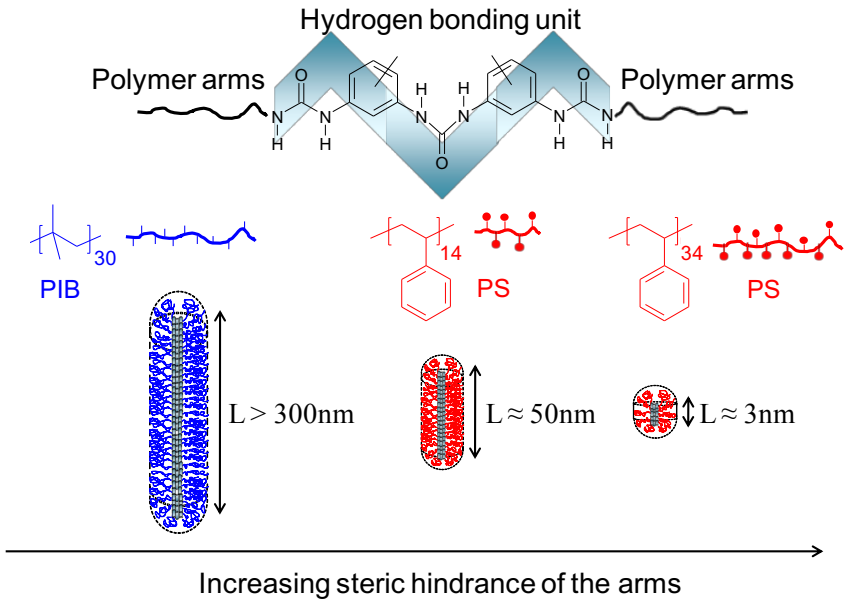

Self-assembly of polymer-decorated trisureas into supramolecular bottle-brushes.